A typical trace is shown in Fig. 2. The trace represents the time development of the imbalance of the bridge after the impulse of photons has created an electron-hole plasma. The total static insertion loss of the device was less than 1.0 dB. The maximum dynamic insertion loss was less than 1 dB. Significant laser induced reflection was not observed, hence we conclude the change in the transmission level is due primarily to plasma related losses.

In Fig. 3, the computed phase shift at $t \approx 0.7$ nsec is plotted as a function of density. The numerical values of the phase shift reduced directly from the data are also plotted as a function of the total available pair-producing energy in a single pulse of light. The scale is indicated along the upper abscissa. The correspondence between the data and the theoretically predicted curve is quite good. The scatter in the data points yields the relative error in our measurements. The uncertainty in the absolute scales is on the order of $\pm 5\%$.

The sensitivity of our model with respect to variations in the depth d of the injected sheet of plasma was also considered. Referring to Fig. 3, the overall agreement between the data and the theoretical curve calculated for $d = 1\ \mu$m is very good. The depth $d = 1\ \mu$m corresponds closely to the depth that one expects the initially thin plasma to expand to in the $t = 0.7$ nsec if the diffusion processes were ambipolar. In addition, curves computed for other values of d strongly suggest that our model is very sensitive to the depth of the plasma. The curves also indicate a nearly two order of magnitude decrease in the total number of carriers n required to cause a maximum normalized phase shift. Additional calculations[8] predict a further order of magnitude reduction in n for similar waveguides designed to operate closer to the cutoff frequency. More precise observations concerning the effects of plasma spatial dimensions awaits further refinement of the model and measurements.

The principal conclusions of this work are, therefore, that a fundamental control operation for millimeter waves, phase shifting, can be effectively achieved using optical techniques and that these techniques offer the additional potential to precisely determine the operationally related fundamental mechanisms of the intervening electron-hole plasma.

The authors wish to thank E. Swiggard and C. Young of the Naval Research Laboratory and Professor C.L. Chen of Purdue University for their cooperation in this project. This work was supported nad carried out at the Naval Research Laboratory.

[1]I.P. Kaminow, J.R. Carruthers, E.H. Turner, L.W. Stulz, Appl. Phys. Lett. **22**, 540 (1973).
[2]R.V. Garver, *Microwave Diode Control Devices* (Artech House, 1976), Chap. 10.
[3]H. Jacobs and M.M. Chrepta, IEEE Trans. **MTT-22**, 411 (1978).
[4]E.A.J. Marcatili, Bell Syst. Tech. J. **48**, 2074 (1969).
[5]C. Kittel, *Introduction to Solid State Physics* (Wiley, New York, 1977).
[6]J.N. Polsky and G.L. Mitchell, J. Opt. Soc. Am. **64**, 274 (1974).
[7]C.L. Chen (private communication).
[8]Chi H. Lee, P. Mak, and A.P. DeFonzo (unpublished).

(InGa) (AsP)/InP embedded mesa stripe lasers

F. C. Prince, N. B. Patel, and D. J. Bull
IFGW-Unicamp/13.100 Campinas/SP/Brasil

(Received 14 June 1979; accepted for publication 7 August 1979)

A structure to avoid nonlinearities in the light-output versus current is proposed in long wavelength lasers of InGaAsP. This structure is very similar to a channeled-substrate planar laser in GaAlAs system. As in the GaAs lasers, nonlinearities are significantly reduced by introducing a built-in passive wave-guiding mechanism.

PACS numbers: 42.55.Px, 42.80.Lt, 85.60.Jb

It has been demonstrated[1,2] in GaAlAs/GaAs DH (double heterostructure) lasers that by introducing in the active region a built-in guiding mechanism along the junction plane with an effective difference in the refractive index larger than 1×10^{-3}, the transverse mode is stabilized to more than 10-mW output power. There are many ways to introduce this built-in refractive index, such as deep-planar lasers,[2] strip-loaded waveguide lasers,[3] transverse junction stripe lasers,[4] channeled-substrate planar lasers,[1] and others. Recently some of these structures have been made in the InGaAsP system.[5-8]

The construction of special structures in the InP system is more difficult due to thermal etching of the substrate before growth. For fabrication of the embedded mesa stripe lasers two runs are necessary: first, a normal three layers DH wafer is grown on a (111)*B* InP substrate (*n*-type tin doped at 2×10^{18} cm^{-3}). The first layer is 7-μm-thick InP, Sn doped at 4×10^{17} cm^{-3}, the second layer is the quaternary $In_{1-x}Ga_xAs_yP_{1-y}$ 0.2 μm thick, and the third layer is 2.0-μm-thick InP, Zn doped at 3×10^{18} cm^{-3}.

Before the second run, 5–8-μm-wide silicon dioxide stripes are defined on top of the wafer by usual photoresist techniques. The wafer is then put back in the LPE growth

 0003-6951/79/200577-04$00.50

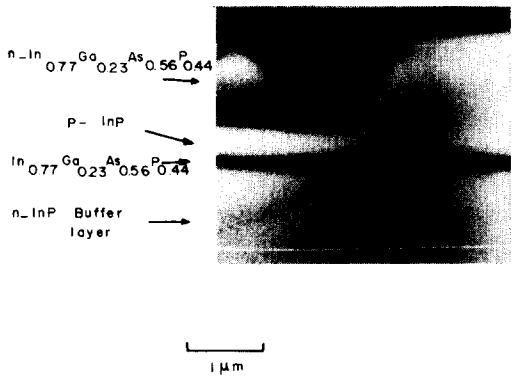

FIG. 1. SEM photograph of cross section of embedded mesa stripe laser.

system where it is reacted with an undersaturated (10 °C) melt of InP.

The meltback is allowed to take place for 10 sec,[7] so that the top (InP) layer is etched down to a thickness of 0.3 μm except under the oxide stripe where a mesa is left. Next, a undoped quaternary layer of composition identical to the active layer is grown so that it fills in the regions etched away by the previous melt. Since this layer is nominally *n* type (5×10^{16} cm^{-3}), it serves to isolate the *p*-type mesa as a stripe contact.

The layers were grown by a supercooling[9] technique, and particularly the quaternary layers were grown with 10 °C of supercooling at 640 °C. The solid composition was determined in a similarly grown 2.0-μm-thick quaternary layer. It was also measured in the final layer of the wafer by electron microprobe analysis[10] resulting in $x = 0.23$ and $y = 0.56$. Also the lattice mismatch was determined by x ray giving $\Delta a/a = 0.07\%$.

Contacts were made by evaporating Au/Zn and Au/Sn onto *p* and *n* sides respectively, and alloying at 450 °C in a hydrogen atmosphere for 30 sec. Devices were made by cleaving bars of 300-μm width and sawing between the stripes. For comparison, lasers were also made from identically grown three-layer structures on which normal silicon dioxide stripe contacts were applied.

A cross-sectional SEM photograph of a EMS laser is shown in Fig. 1. We can see that the etchback leaves the mesa in the trapezoidal form. We note that this form appears only when the substrate is (111)*B*. When we use (100) substrate, the mesa shoulder is not so sharp.

The shoulder width varies in the 7–9-μm range, and also the thickness of the *p*-InP layer which is left varies between 0.2 and 0.5 μm. In the regions far from the mesa shoulders the *p*-InP layer can reach 1.0-μm thickness. This nonuniformity is of course due to the meltback step in the fabrication process.

The values of these parameters were chosen to be similar to those used in the CSP laser[1] due to unavailability of data which would allow us to calculate optimum values for our laser. Since the results obtained are satisfactory as far as avoiding the "kink" is concerned, the optimum values of these parameters should not be very different from those chosen by us.

Light-output–vs–current characteristics obtained under pulsed operation are shown in Fig. 2. The room-temperature threshold current density is 10–12 kA/cm^2. This high value may be due to two reasons. First, the junction position determined by EBIC measurements is 0.3 μm away from the active layer, due to Zn diffusion, (within the buffer layer) so that the holes are not confined in 0.2-μm quaternary layer. Second, because of this Zn diffusion, the active layer is heavily doped (at least 10^{18} cm^{-3} because the top layer is 3×10^{18} cm^{-3}) so that the free-carrier absorption is high. Together with these facts, we have a normal increase in the threshold current density due to a top absorbing/confining layer.

The observed external quantum efficiency under pulsed operation is typically 30%.

Near-field and far-field intensity distribution along the junction plane are shown in Figs. 3(a) and 3(b), respectively, at five different injection levels. We can see that the radiation patterns are unchanged with increasing injection. The full width at half-maximum (FWHM) of the far field is 15° and the near-field spot size at half-power is 3.6 μm. The shoulder width for this device is 7 μm, the active layer is 0.2 μm, and the thickness of the top transparent InP layer near the shoulder is 0.3 μm. For comparison, a typical near field obtained from the SiO_2 striped laser is shown in Fig. 4. A clear improvement in stabilization of the transverse mode can be seen for the EMS laser.

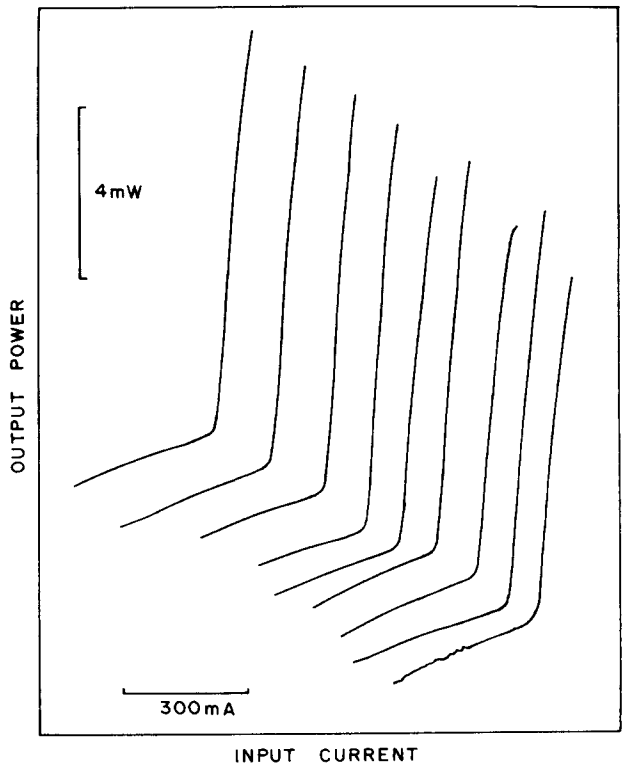

FIG. 2. Light-output power versus current of the EMS lasers for randomly chosen nine lasers. The curves are translated horizontally and vertically to not overlap. Active layer is 0.2 μm, the shoulder width is 7–9 μm, and adjacent transparent InP layer near the shoulder is 0.3–0.5 μm.

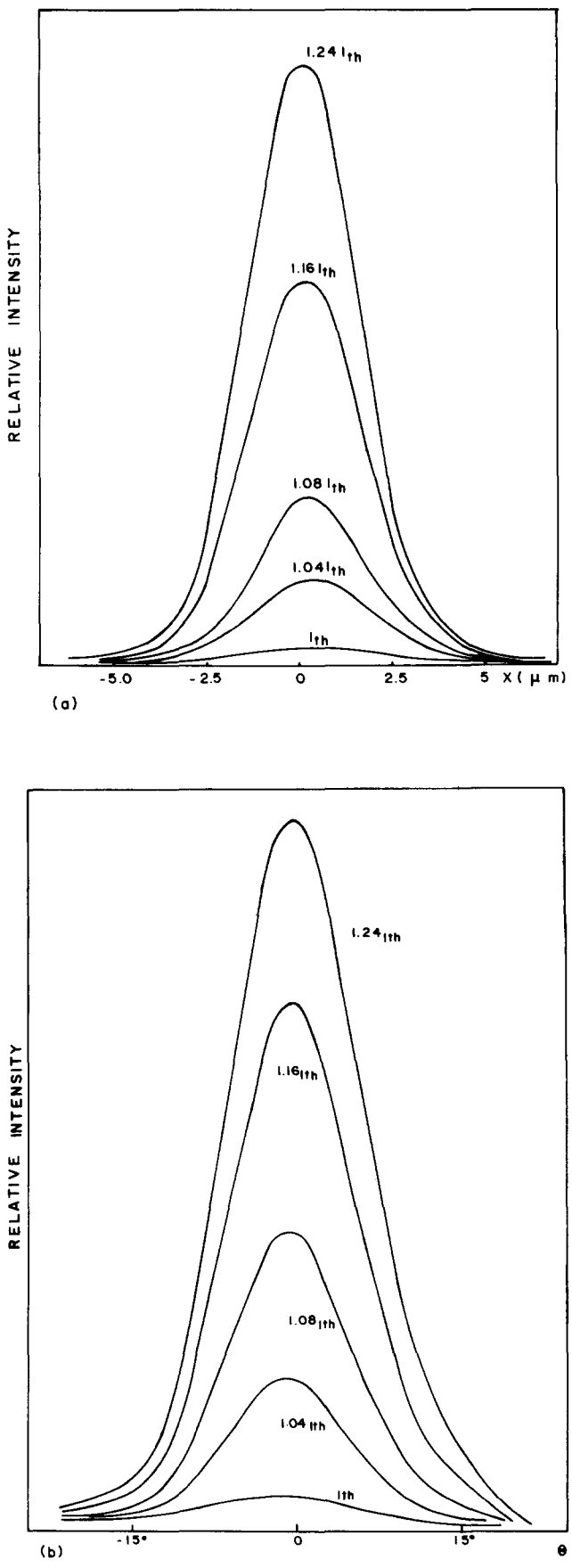

FIG. 3. (a) Near field along the junction plane of EMS laser. Near-field spot width at half-power is 3.6 μm. (b) Far field along the junction plane of EMS laser. FWHM is 15°.

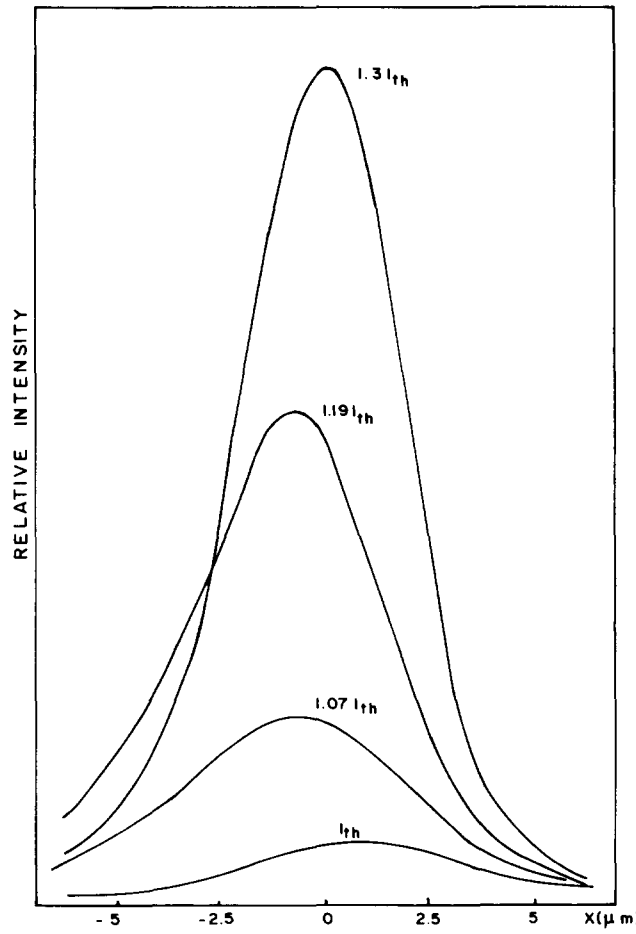

FIG. 4. Near field of SiO_2 striped laser. Stripe width is 12 μm.

Lasing spectra of the EMS lasers were also investigated. The lasing wavelength is 1.3 μm, and a large fraction of the lasing output occurs in a single longitudinal mode. When the current increases, a jump to longer wavelength mode is observed. This fact is attributed to the heating of the active region[11] by the injected carriers.

No emission was found in the 0.95-μm-wavelength region. We explain this fact by the following: the electrons, injected in the *p-n* junction within the buffer InP layer, diffuse and fall in the potential well that exists due to the energy gap E_g difference of the InP and InGaAsP layers, and then recombine giving a photon of energy near the value of the energy gap of the quaternary layer.[6]

In summary, a waveguide structure similar to CSP[1] lasers was fabricated in the InGaAsP system. Good linearity in the light-output–vs–current and stabilization of transverse mode was obtained. Also, almost single longitudinal mode occurs in the EMS lasers, which, though not an advantage at 1.3 μm for fiberoptic system, would be advantageous at longer wavelengths. The main advantage of this structure is that by making use of the quaternary *n*-type layer on the top, and of a very shallow Zn diffusion, we can make good Ohmic contacts.

The authors are grateful to Dr. Wolfgang Rühle and Dr. J. Harris, Jr. for useful discussions, to J.L. Gonçalves for help in crystal growth, to A. Celso Ramos for SEM evaluations, and to TELEBRÁS for financial support.

[1]K. Aiki, M. Nakamura, T. Kuroda, J. Umeda, R. Ito, N. Chinone, and M. Maeda, IEEE J. Quantum Electron. **QE-14**, 89 (1978).
[2]H. Yonezu, Y. Matsumoto, T. Shinohara, I. Sakuma, T. Suzuki, K. Kobayashi, R. Lang, Y. Nannichi, and I. Hayashi, Jpn. J. Appl. Phys. **16**, 209 (1977).
[3]H. Kawaguchi and T. Kawakami, IEEE J. Quantum Electron. **QE-13**, 556 (1977).
[4]H. Namizaki, H. Kan, M. Ishii, and A. Ito, J. Appl. Phys. **45**, 2785 (1974).
[5]J.J. Hsieh, IEEE Semiconductor Laser Conference San Francisco, 1978 (unpublished).
[6]D.J. Bull, N.B. Patel, F.C. Prince, and Y. Nannichi, Special Issue IEEE J. Quantum Electron., Aug. (1979).
[7]H. Kano, K. Oe, S. Ando, and K. Sugiyama, Jpn. J. Appl. Phys. **17**, 1887 (1978).
[8]J.J. Hsieh and C.C. Shen, Appl. Phys. Lett. **30**, 429 (1977).
[9]J.J. Hsieh, J. Cryst. Growth **27**, 49 (1974).
[10]J.W. Colby, Proc. Sixth Nat. Conf. on Electron Probe Analysis, 1971 Vol. 17 (unpublished).
[11]M. Nakamura, K. Aiki, N. Chinone, R. Ito, and J. Umeda, J. Appl. Phys. **49**, 4644 (1978).

The isotope shift in the 2^2P states of lithium and spatially resolved laser-induced fluorescence

R. Mariella, Jr.
Allied Chemical Co., Photon Chemistry Department, P.O. Box 1021R Morristown, New Jersey 07960

(Received 27 June 1979; accepted for publication 27 June 1979)

Spatially resolved laser-induced fluorescence has been used to observe and measure the isotope shift for atomic lithium in the $2^2P \leftarrow 2^2S$ transitions. A modified saturated absorption spectrum was also obtained for the "overlapping" transitions. The ^{7}Li-^{6}Li isotope shift in the absence of fine and hyperfine splittings is calculated to be 10532 ± 5 MHz.

PACS numbers: 32.50. + d, 28.60. + s

The technique of spatially resolved laser-induced fluorescence (SRLIF), described in some detail by Levy, Wharton, and Smalley[1] and used by them to control linewidths and measure lifetimes in their studies of NO_2 and I_2, can be employed in a variety of ways with atomic or molecular beams. The particular application in the present study is the exploitation of the inhomogeneous nature of the Doppler width to make spectroscopic measurements. Briefly, a well-collimated laser beam crosses an atomic (or molecular) beam in a nominally perpendicular configuration, but the finite divergence of the atomic beam leaves a finite Doppler width as well. The collision-free nature of the atomic beam flow, which emanates essentially from a point source, produces a simple correspondence between the physical location of an atom which is traversing the laser beam and the angle of intersection θ of its velocity vector with the direction of light propagation, $\theta = \text{arccot}(X/H)$, where H is the distance from the oven orifice to the laser beam and X is the distance of an atom from the center of the atomic beam (see Fig. 1). For atoms with a single speed v and absorbing light of wavelength λ, the Doppler shift $\Delta\nu_D$ is calculated by $\Delta\nu_D = -(v\cos\theta)/\lambda$. (The spread of atomic or molecular speeds from an effusive source and its finite orifice size introduces only a slight broadening if H is much larger than the orifice diameter and if θ is near 90°.) Conversely, one can adjust the angle θ, and hence the position X, of on-resonance atoms by adjusting the wavelength of the exciting light. If the bandwidth of the exciting light and the lifetime-limited linewidth of the transition are less than the residual Doppler width, assuming that problems from transit-time broadening and power broadening have been avoided, then the fluorescence will be localized to a fraction of the region of overlap between the atomic beam and the laser beam. The case is shown in Fig. 1 where the exciting light falls midway between two hyperfine transitions whose frequency separation is less than the residual Doppler width.

In the present study a lithium beam with a full divergence of $3\frac{1}{2}°$ was probed on the $2^2P \leftarrow 2^2S$ transition with a Coherent Radiation Model 599 single-mode rhodamine 640 (Exciton Chemical Co.) dye laser operating near 670.791 nm. A conventional two-chamber effusive oven[2] was operated typically at 525 °C (the lithium vapor pressure[3] is 7.5×10^{-3} mm Hg at this temperature) with a 1-mm-diam. collimator placed 1.6 cm above the 1-mm-diam. oven orifice. The 1.2-mm-diam. laser beam passed through the

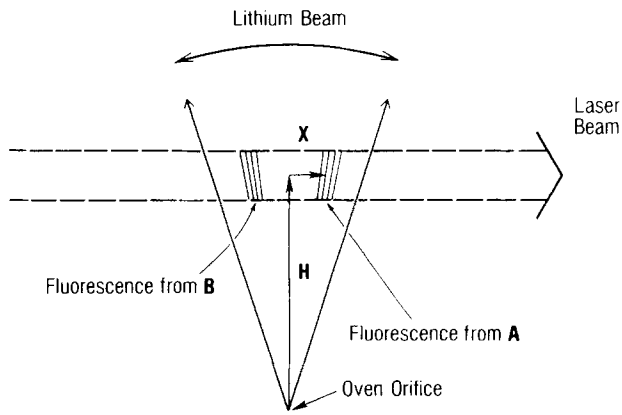

FIG. 1. Schematic illustration of the spatially resolved fluorescence which is seen when the laser wavelength is midway between the transitions labeled A and B in Figs. 2 and 3. The symbols H and X are defined in the text. The atomic beam divergence and the width of the fluorescing spots are exaggerated.

 0003-6951/79/200580-03$00.50